NeuroImage 120 (2015) 254–265

Contents lists available at ScienceDirect

NeuroImage

journal homepage: www.elsevier.com/locate/ynimg

Microstructure of the superior longitudinal fasciculus predicts stimulation-induced interference with on-line motor control

Borja Rodríguez-Herreros [a,c,h,1], Julià L. Amengual [b,c,1], Ane Gurtubay-Antolín [a,b], Lars Richter [d], Philipp Jauer [d], Christian Erdmann [c,e], Achim Schweikard [d], Joan López-Moliner [a,f], Antoni Rodríguez-Fornells [a,b,f,2], Thomas F. Münte [c,g,*,2]

[a] Department of Basic Psychology, Universitat de Barcelona, 08035 Barcelona, Spain
[b] Cognition and Brain Plasticity Unit, Bellvitge Research Biomedical Institute (IDIBELL), Hospitalet de Llobregat, 08907 Barcelona, Spain
[c] Department of Neurology, University of Lübeck, 23538 Lübeck, Germany
[d] Institute for Robotics and Cognitive Systems, University of Lübeck, 23538 Lübeck, Germany
[e] Department of Neuroradiology, University of Lübeck, 23538 Lübeck, Germany
[f] Institució Catalana de Recerca i Estudis Avançats (ICREA), 08010 Barcelona, Spain
[g] Institute of Psychology II, University of Lübeck, 23538 Lübeck, Germany
[h] LREN & Service of Medical Genetics, Centre Hospitalier Universitaire Vaudois, Université de Lausanne, 1011 Lausanne, Switzerland

ARTICLE INFO

Article history:
Received 29 January 2015
Accepted 25 June 2015
Available online 2 July 2015

Keywords:
Reaching
On-line motor control
Repetitive TMS
Diffusion tensor imaging
Superior longitudinal fasciculus II

ABSTRACT

A cortical visuomotor network, comprising the medial intraparietal sulcus (mIPS) and the dorsal premotor area (PMd), encodes the sensorimotor transformations required for the on-line control of reaching movements. How information is transmitted between these two regions and which pathways are involved, are less clear. Here, we use a multimodal approach combining repetitive transcranial magnetic stimulation (rTMS) and diffusion tensor imaging (DTI) to investigate whether structural connectivity in the 'reaching' circuit is associated to variations in the ability to control and update a movement. We induced a transient disruption of the neural processes underlying on-line motor adjustments by applying 1 Hz rTMS over the mIPS. After the stimulation protocol, participants globally showed a reduction of the number of corrective trajectories during a reaching task that included unexpected visual perturbations. A voxel-based analysis revealed that participants exhibiting higher fractional anisotropy (FA) in the second branch of the superior longitudinal fasciculus (SLF II) suffered less rTMS-induced behavioral impact. These results indicate that the microstructural features of the white matter bundles within the parieto-frontal 'reaching' circuit play a prominent role when action reprogramming is interfered. Moreover, our study suggests that the structural alignment and cohesion of the white matter tracts might be used as a predictor to characterize the extent of motor impairments.

Introduction

One of the main functions of the brain is the on-line monitoring and control of movements. The apparent ease with which we perform even complex movements belies the abundant neural operations that are involved in this process, including several hierarchical levels of the visual and the motor system. Numerous studies have implicated the posterior parietal cortex (PPC) in the on-line control of a movement after its initiation (see Andersen et al., 1997 for review). The role of the intraparietal sulcus (IPS), a specific subregion of the PPC, in monitoring visually-guided grasping (Tunik et al., 2007) and reaching movements (Clower et al., 1996) has been widely supported by neurophysiological (Sakata et al., 1995) and brain imaging evidence (Culham et al., 2003; Frey et al., 2005). Seminal studies in monkeys suggest that parieto-frontal circuits that link the medial intraparietal sulcus (MIP in monkeys) and the dorsal premotor cortex (PMd) are thought to sustain the visuomotor transformations for the on-line control of reaching (Caminiti et al., 1996; Johnson and Ferraina, 1996; Johnson et al., 1993). In human neuroimaging studies, extensive activation of a putative homologue of MIP area, called medial intraparietal sulcus (mIPS), and the PMd have been reported during reaching and pointing movements (Colebatch et al., 1991; Desmurget et al., 2001; Kertzman et al., 1997). Many mIPS neurons discharge with changes in the location of the target relative to the hand, i.e., they scale with the extent of the 'motor error' (Andersen and Buneo, 2002). They respond not only before movement onset but also during its execution, which allows the mIPS to integrate sensory input with efference copies of

* Corresponding author at: Department of Neurology, University of Lübeck, 23538 Lübeck, Germany.
E-mail address: thomas.muente@neuro.uni-luebeck.de (T.F. Münte).
[1] These authors contributed equally to this work.
[2] These authors share senior authorship.

http://dx.doi.org/10.1016/j.neuroimage.2015.06.070
1053-8119/

outgoing motor commands. This arrangement suggests that the mIPS is a key region that provides PMd with a constant flow of neural signals associated with a continuously updated estimate of the motor error. Nonetheless, how mIPS transfers to PMd the sensorimotor information required for an appropriate supervision of reaching and which structures are used remain to be elucidated.

Just as the size and capacity of roadways can regulate the flow of traffic between different cities, the architecture of white matter (WM) tracts between different brain regions determines the amount and quality of information transmitted between these regions (Behrens and Johansen-Berg, 2005). Previous neuroanatomical studies revealed activity in the ventral aspect of the mIPS as well as the rostral part of PMd when updating a pre-specified motor instruction, suggesting a cortico-cortical parieto-frontal pathway between these areas (Johnson and Ferraina, 1996; Wise et al., 1997). In this sense, the superior longitudinal fasciculus (SLF) is the major cortical association fiber pathway linking parietal and frontal cortices in both humans and monkeys. It is subdivided into three different components (Petrides and Pandya, 1984): In humans, SLF I is medially situated in the white matter of the superior parietal lobule (Brodmann area (BA) 5) and the superior frontal gyrus (BA 8, 9, 32) (Makris et al., 2005). The second branch of the superior longitudinal fasciculus (SLF II) originates from the intraparietal sulcus and inferior parietal lobule and terminates in the superior sector of BA 6 (PMd) and the posterior regions of the inferior frontal gyrus (Schmahmann et al., 2007; Thiebaut de Schotten et al., 2012). Finally, the SLF III is further lateral and ventral and is located in the white matter of the parietal and frontal operculum (Schmahmann and Pandya, 2006). The SLF II has thus been postulated as an important neural tract within the premotor-parietal network that connects the IPS and the PMd (Boorman et al., 2007; Thiebaut de Schotten et al., 2012). In this regard, virtual *in vivo* dissections using diffusion imaging tractography have associated the anatomical asymmetry of the SLF II, unlike the SLF I and III, to the behavioral performance on visuospatial attention tasks (Thiebaut de Schotten et al., 2011).

In the present study, we tested whether the properties of the SLF II modulate the degree of interference on the ability to update a movement. We tested this hypothesis by using high-resolution diffusion tensor imaging (DTI) in combination with repetitive transcranial magnetic stimulation (rTMS). The rationale for the use of brain stimulation relies on the fact that purely baseline behavioral measures may encompass the integrated function of multiple brain regions. Rather, the specific impact of rTMS application in on-line motor control could be a more informative and isolated measure of a certain brain function with which to compare structural parameters (Boorman et al., 2007). A brief burst of TMS pulses over the mIPS has been shown to induce short-lived disruptions of the capacity to correct reaching movements (Della-Maggiore et al., 2004; Desmurget et al., 1999). There are an overwhelming number of studies supporting that the application of trains of rTMS can either increase or decrease the cortical excitability of the targeted region depending on the stimulation conditions, and consequently affect the behavior supported by this brain area (see Siebner et al., 2009 for review). Moreover, modulation of the neural activity is not confined to the target area but can also extent to other connected brain regions (Gerschlager et al., 2001; Siebner et al., 2000; Wassermann et al., 1998). With the advent of in vivo DTI quantitative metrics based on water diffusion, neuroimaging studies have been able to evaluate morphological changes in microstructural architecture (Darquie et al., 2001; Kimiwada et al., 2006; Le Bihan et al., 2006). By measuring fractional anisotropy (FA) — a measure which is thought to reflect the integrity and fiber density of WM fibers — we predict that an rTMS-induced breakdown of the mIPS function will affect the ability to adjust ongoing reaching movements, and that this behavioral impact might hint in the structural properties of parieto-frontal fibers linking mIPS with PMd.

Materials and methods

Participants

Twenty-four healthy right-handed volunteers (12 women; mean age 26.6 ± 4.9 years) participated in this study. All subjects were naïve with respect to the experimental procedures and the hypothesis of the study. Participants had normal or corrected-to-normal visual acuity and reported neither previous nor current neuropsychiatric disorders. Prior to their inclusion in the study, participants provided written informed consent. The study was performed according with the declaration of Helsinki and was approved by the ethics committee of the University of Lübeck. All participants were screened for MRI and TMS compatibility (Machii et al., 2006). The Edinburgh handedness inventory was required to assess right-handedness (Oldfield, 1971). All participants were paid for their participation.

Apparatus and data acquisition

An overview of the experimental setup is shown in Fig. 1. Subjects sat at a table that was 45–50 cm below the eyes. Visual stimuli were generated by an Apple MacBook 2 GHz Quad-Core and displayed on a 17 in. LCD monitor with a refresh rate of 120 Hz and a resolution of 1280 × 1024 pixels (43.3 cm of diagonal viewing size). A 3D marker with infrared LEDs was attached to the index finger tip of the hand in order to track the finger's spatial position during reaching movements. The marker was connected to and tracked by a high-speed real-time optical tracking system (Atracsys accuTrack 250, Atracsys LLC, Inc.). The spatial resolution was 0.01 mm in each spatial axis. The sampling rate of the recording was set to 200 Hz. For each movement, finger coordinates were recorded from 200 ms before the stimulus was presented on the screen (see below for a full description of the stimuli), and ended 300 ms after the end of the movement. Missing samples in recorded coordinates due to erratic orientations of the infrared marker were interpolated off-line (Tunik et al., 2005) by using spline functions (Liu and McMillan, 2006). Time series of the recorded individual position coordinates were processed with a low-pass Butterworth filter (cutoff frequency of 6 Hz) for further analysis (Mason et al., 2001; Rodriguez-Herreros and Lopez-Moliner, 2011). Velocity was derived from the smoothed time series of the marker's position by first numerical differentiation.

Stimuli and procedure

The experimental task (Adjusting Condition, AC) consisted in performing a reaching movement towards a visual target located on the screen. Prior to the initiation of the trial, participants were required to move the index finger to a red bulge situated 30 cm in front of the screen and localizable by sensory tactile feedback. After 1000 ms with the finger placed at this starting point, a small white fixation point was automatically shown as a warning signal in the center of the screen (Fig. 1A). Subjects were asked to fixate the point until a target appeared in the center of the screen (30 mm in diameter green dot), 30 cm above the surface of the table. In order to avoid participants from predicting the target onset, a variable foreperiod (300 or 800 ms) between the appearance of the fixation point and the target onset was used. Trials without (66%) and with (34%) displacement were presented in pseudorandom order. In undisplaced trials, the target remained static in the center of the screen. In contrast, displaced trials showed an unexpected lateral displacement of the target position at the time of the movement onset, 10 cm lateral to the initial position. The displacement was timed at the movement onset to assure that participants did not have relevant information about the final position of the target during the initial planning of the movement. To this aim, the movement onset was detected by a specific velocity threshold (see Behavioral analysis section) obtained from the infrared data. To discard trials

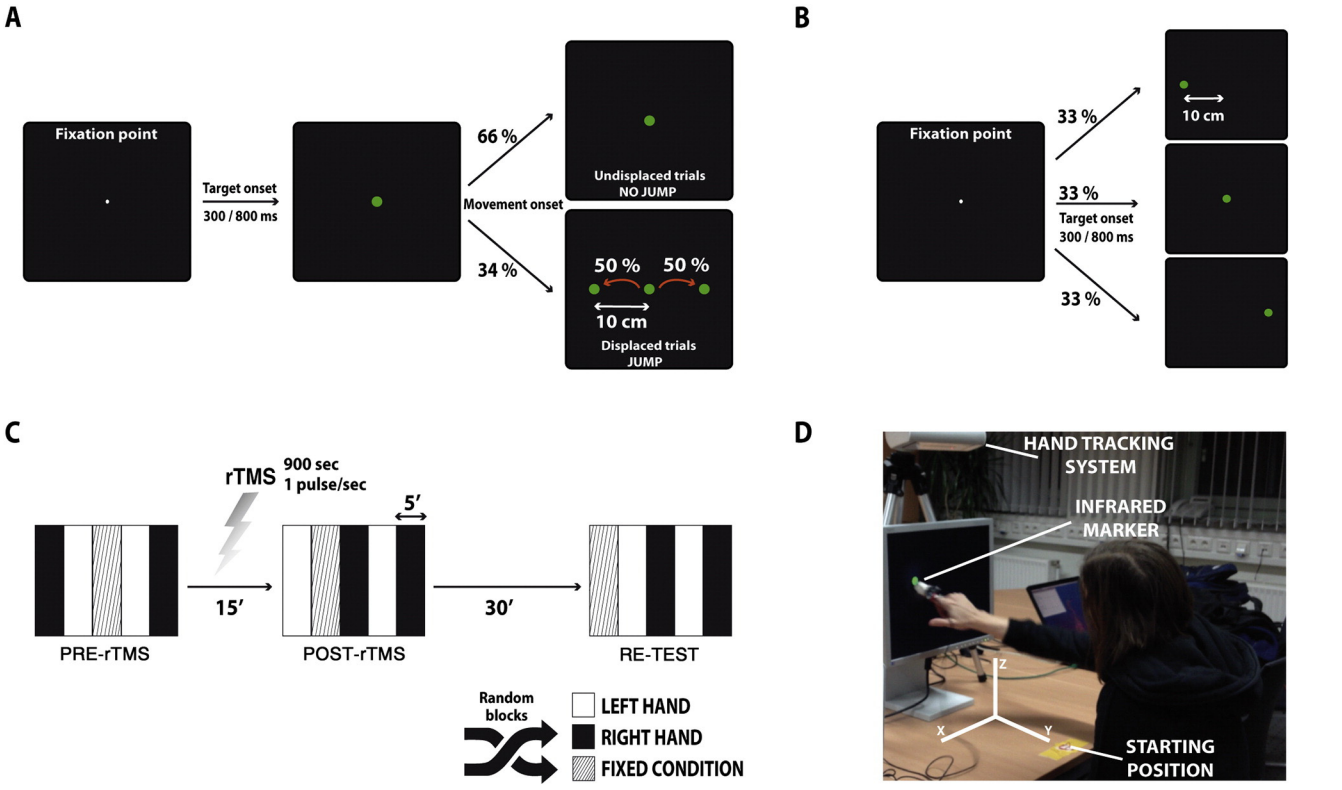

Fig. 1. Visual display of the adjusting condition (AC) (A) and the fixed condition (FC) (B). C. Time course of the experimental events. Each block lasted around 5 min with 1 min of rest between each, so an entire session was approximately 30 min. Blocks were randomly distributed within each session. D. Illustration of an on-line adjustment after a displaced trial in the adjusting condition. A three-dimensional reference coordinate system was established with the center of the lateral axis ($x = 0$) determined by the center of the screen, and the zero value of the longitudinal axis ($y = 0$) defined by the hand starting point. Origin of the vertical axis (z) was the surface of the table. As a result, the origin of coordinates was settled as the hand starting position. The distance between the virtual target and the hand initial position was approximately 42 cm.

with long reaction times, a warning sound was provided if the velocity threshold was not exceeded within 500 ms after the target onset. Participants were instructed to hit the target with the index finger. When the target was displaced, participants had to modify the hand trajectory to the final target location. Participants were also instructed to start and perform the movement as fast as possible. The target was presented for 1000 ms. At the end of the reaching movement, participants brought their hand back to the starting point.

An additional condition (Fixed Condition, FC) was introduced to rule out that rTMS stimulation affected the visual processing of the target location (Fig. 1B). FC differed from AC in that the target directly appeared either in the center or in one of the two lateral locations with no displacement at the movement onset. Hence, participants already had the information about the final position of the target during the planning phase of the movement. In FC, central and lateral target locations appeared in pseudorandom order with equal probability.

Experimental design

The experimental design comprised three different sessions (Fig. 1C): a baseline measurement (Pre-rTMS); immediately after the application of the rTMS (Post-rTMS) and 30 min after the end of the Post-rTMS measurement (Re-Test). The rTMS protocol lasted 15 min and participants performed the task immediately thereafter. The duration of each session was approximately 30 min. Once the participants finished the Post-rTMS session, they rested in the room for 30 minutes. Only after these additional 30 min of rest, they performed the final Re-Test session, that is, 60 min after the end of the rTMS protocol. Each session was composed of four blocks of the AC and one block of the FC with 100 trials each. Between each block, 1 min of rest was given. Two blocks of the AC were performed with the right hand and the other two with the left hand. The single block of the FC was performed with the right hand. The order of blocks was counterbalanced across subjects for each session. Therefore, each participant completed 1500 trials: 1200 trials of the AC and 300 trials of the FC. Before the experiment started, subjects performed 40–50 practice trials until they got familiar with the task. Participants were instructed not to move their trunk with respect to the chair during a entire block. Head movements were allowed to avoid that subject's behavior could be different than in natural conditions (Steinman et al., 1990) (Fig. 1D).

TMS protocol

A robotized TMS system with active motion compensation was used for accurate and consistent stimulation (Matthaus, 2008; Richter, 2013). Stimulation pulses were applied using a MCF-B65 figure-of-eight coil (9 cm each wing) designed for focal stimulation. The coil was connected to a MagPro X100 MagOption stimulator (MagVenture A/S, Farum, Denmark) for biphasic stimulation, and was attached to the end effector of the articulated arm of an Adept Viper s850 serial six joint robot (Adept Technology, Inc., Livermoore, CA, USA), ensuring an accurate placement of the coil. The robot was driven by a standard PC with an image-guided robot-control software. A Polaris stereo-optic infrared tracking system (Northern Digital Inc., Waterloo, Ontario, Canada) recorded the head movements by tracking a marker consisting of five reflective spheres that was placed at the subject's forehead with a headband. The headband position was continuously tracked during the stimulation for head navigation. Likewise, a pointer with identical passive reflective marker spheres was utilized to acquire an individual 3D digital outline of the participant's head by recording approximately 500 surface points and three standard landmarks (lateral orbital rims and tip of the nose). We calibrated the tracking system setting the robot position as a reference of coordinates (Richter et al., 2011). As a result, real-time robotic motion compensation of the head movements

was rendered by its respective coil motion. This methodological advantage assures an accurate location of the stimulation region throughout the entire rTMS protocol. In contrast to hand-held approaches, this montage guaranteed to keep the initial orientation and strength throughout the entire experiment by adapting the coil motion to unrestrained head movements (Richter et al., 2013).

Prior to the rTMS procedures, motor evoked potentials (MEPs) were recorded attaching surface Ag/Cl electrodes to the skin over the right first dorsal interosseous (FDI) muscle in a belly-tendon setting. Electromyographic (EMG) data was recorded by a 2-channel DanTec Keypoint Portable system (Alpine Biomed Aps, Skovlunde, Denmark) at a sampling rate of 50 kHz. The EMG signal was processed with a (10 Hz–10 kHz) band-pass filter. First, resting (rMT) and active (aMT) motor thresholds were measured for each participant. For this, the coil was positioned over the hand area of the left primary motor cortex. The rMT was defined as the minimum stimulator intensity at which 50% of pulses induced an MEP of at least 0.05 mV of amplitude in the relaxed FDI muscle (Rossini et al., 1994). The aMT was defined as the minimum stimulation intensity at which 50% of pulses induced an MEP of at least 0.2 mV during a voluntary contraction of the FDI (Huang et al., 2005). Second, the rTMS protocol consisted on a train of 900 pulses delivered with a frequency of 1 Hz. During the application of the pulses, subjects maintained a relaxed posture and kept their eyes closed. The intensity of the magnetic stimulation was fixed to 60% of the maximum stimulator output (MSO), following several previous TMS studies on PPC (Buelte et al., 2008; Machii et al., 2006; Vesia et al., 2010). After the stimulation, only three subjects reported neck pain, which they all attributed to postural reasons.

Localization of stimulation sites

The mIPS of the left hemisphere was chosen for stimulation, located over the midposterior junction of the IPS, caudal to the aIPS (Desmurget et al., 1999; Glover et al., 2005; Prado et al., 2005; Vesia et al., 2010). A T1-weighted high-resolution 3D structural MRI (3T Philips Achieva whole-body scanner) was obtained for each participant. For all participants, average normalized coordinates of the targeted area were reported according to standardized stereotaxic space (Rey et al., 1988). In particular, the left mIPS was determined by the medial bank of the intraparietal sulcus over the midposterior junction [group mean ± SD: MNI coordinates, $x = -24.8 \pm 3.2$, $y = -58.4 \pm 6.8$, $z = 49.8 \pm 7.1$]. The coordinates were concurrent with other TMS (Davare et al., 2012; Vesia et al., 2010) and brain imaging (Blangero et al., 2009; Grefkes et al., 2004; Prado et al., 2005) studies. The coordinates were translated to the robotic software for localization of the appropriate stimulation region on the subject's scalp. The orientation of the coil was tangentially to the cortical surface and positioned 45° with respect to the sagittal plane of the cranial MRI data. Direction of the current in the coil was anteroposterior.

DTI acquisition and image processing

Whole-brain diffusion magnetic resonance imaging (dMRI) using a diffusion tensor spin-echo planar imaging sequence was acquired with the following scanning parameters: voxel size of $2 \times 2 \times 2$ mm, matrix of 112×112, 70 slices with 2 mm-thick and no gap, TE = 60 ms, TR = 7582 ms, EPI factor = 59, field of view = 224 mm, bandwidth = 2743.6 Hz, b-value = 800 s/mm^2. One single run of 32 diffusion-weighted directions with one non-diffusion-weighted volume was acquired.

Motion and eddy-current correction were performed using FMRIB's Diffusion Toolbox (FDT), part of the FMRIB Software Library (FSL www.fmrib.ox.ac.uk/fsl/) (Smith et al., 2004; Woolrich et al., 2009). The gradient matrix was then rotated and the structural image was fully-stripped using FSL's Brain Extraction Tool (Smith et al., 2002). Diffusion tensors were reconstructed using the linear least-squares method provided in Diffusion Toolkit (Ruopeng Wang, Van J. Wedeen, TrackVis.org, Martinos Center for Biomedical Imaging, Massachusetts General Hospital). The tensor was spectrally decomposed in order to obtain its eigenvalues and eigenvectors. The fiber direction was assumed to correspond to the principal eigenvector (the eigenvector with the largest eigenvalue). Fractional anisotropy (FA) values were generated from the eigenvalues. FA maps from all participants were registered to an MNI FA template (FMRIB58_FA, MNI152 space) using FNIRT (Andersson et al., 2007a,2007b). FA quantifies the anisotropy in each voxel, with values ranging from 0 (fully isotropic) to 1 (diffusion is favored in one axis and hindered in the remaining two). In degenerated tracts water diffusion is more isotropic, thus, FA decreases substantially compared to normal fiber tracts. WM structural analysis was carried out using Voxel Based Analysis (VBA) (Cámara et al., 2007; Fuentemilla et al., 2009). FA maps were processed using MATLAB 7.8.0 (The MathWorks Inc., Natick, Mass) and Statistical Parametric Mapping software (SPM8; Wellcome Trust Centre for Neuroimaging, London, UK). Normalized images were smoothed by using an isotropic Gaussian smoothing kernel of 6 mm full-width-at-half-maximum (FWHM) to reduce residual inter-individual variability.

Behavioral analysis

For each trial, we obtained three-dimensional spatial coordinates of the position of the index finger. Two types of hand trajectories were established for displaced trials: erroneous trajectories and corrective trajectories. The rationale to define a hand trajectory as corrective or as erroneous was as follows (Fig. 2): (1) we first obtained the distribution of all the finger endpoints for the undisplaced trials by calculating the ellipsoid 95% confidence interval (CI) (Granek et al., 2012; Messier and Kalaska, 1999). Trajectories of displaced trials in which the index-finger endpoint position was within this CI were considered as erroneous trajectories (Pisella et al., 2000). Additionally, since the main instruction provided to participants was to hit the target, we amplified this exclusion criterion by considering also as erroneous the hand trajectories that ended out of the ellipsoid 95% CI formed by the endpoints of the displaced trials. Finally, (2) trajectories that did not pass a velocity

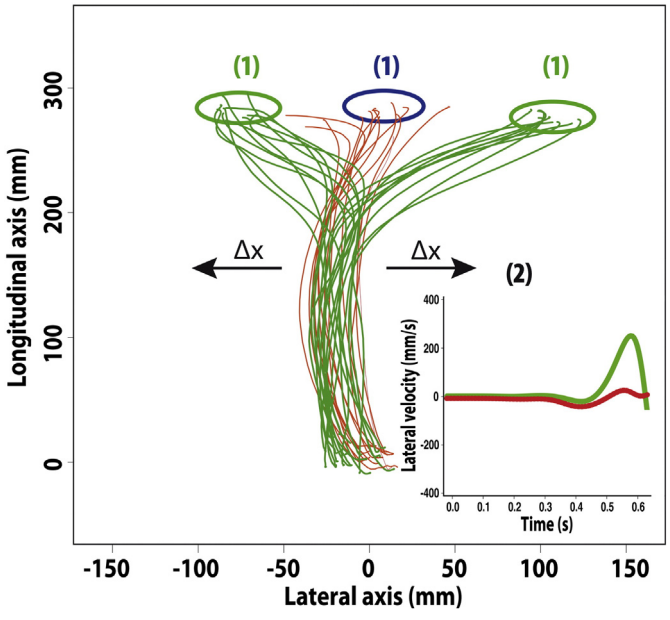

Fig. 2. Criteria to distinguish erroneous (red lines) and corrective (green lines) trajectories. A corrective trajectory must end out of the 95% CI of the undisplaced hand endpoint positions (1, blue ellipse), but also within the 95% CI of the displaced trials (1, green ellipses). (2) Inset: Lateral (x) component of the speed ought to reach a threshold of 100 mm/s during the first 85% of the movement trajectory in order to consider the trajectory as corrective. Zero value of the abscissa axis corresponds to target onset.

threshold of 100 mm/s in its lateral component of the trajectory (Neggers and Bekkering, 2002) during the first 85% of the movement time were also considered as erroneous trajectories. The rest of hand trajectories were defined as corrective. All the CIs were independently calculated for each session, hand and side of the displacement (right, left) in each participant. No overlapping was observed between ellipsoid 95% CI of undisplaced and displaced trials for a given hand within a session.

Kinematic values were inferred from the 3D position of the index finger obtained from the attached infrared markers. We measured the reaction time, movement time, peak velocity and time to peak velocity, deceleration time and correction time as parameters for posterior analysis in both FC and AC. A velocity threshold of 50 mm/s in the longitudinal axis was used to detect the onset and the offset of the movement (Neggers and Bekkering, 2002; van Beers et al., 2004). Reaction time was defined as the time between target onset and movement onset. Movement time was obtained by subtracting the movement onset from the corresponding movement offset. Peak velocity was defined as the maximum speed achieved within the movement time, and time to peak velocity was defined as the time passed between the movement onset and the moment when peak velocity was reached. Deceleration time was obtained by subtracting time to peak velocity from movement time. Correction time was detected with the abovementioned threshold of lateral velocity used as a criterion to detect a corrective movement. The correction time was also expressed as a percentage of the movement time. Finally, we measured the spatial error in the FC as the Euclidian distance between the target location and the endpoint position of the index finger. The systematic error for a given condition was the mean of the spatial errors.

Statistical analysis

In all analyses, the direction of the displacement (left or right) was not considered as a factor, since preliminary analyses revealed a lack of statistical main effects and interactions ($P > 0.34$). Trajectories with more than five consecutive missing samples were removed from the analysis. One participant was discarded due to a high number of missing samples in many trajectories. Prior to analysis, all trials with a reaction time lower than 170 ms or higher than 500 ms were removed. Concerning the movement time, we delimited a valid range from 200 ms to 600 ms (Pisella et al., 2000). Participants with a trial rejection rate higher than 30% were excluded from the analysis.

In the AC, we analyzed the effect of the rTMS on the ability to correct the hand movement in displaced trials by using the error rate (defined as the percentage of erroneous trajectories) for left and right hand in each session. We conducted a 2×3 repeated-measures analysis of variance (ANOVA) with factors session (Pre-rTMS, Post-rTMS, Re-test) and hand (right, left). We also tested for correlations between the error rate of each hand and the rMT and aMT, independently. To ensure that the behavioral aftereffects of the rTMS on the error rate were not attributable to changes of the global motor output, differences in all the above mentioned kinematic parameters were tested using a $3 \times 2 \times 2$ repeated measures ANOVA including session, hand and type of trial (displaced, undisplaced), only considering displaced trials with a corrective trajectory (Boulinguez et al., 2001). Erroneous trajectories were removed from the kinematic analysis due to noisy profiles. An analogous analysis was carried out for the reaction time but omitting the 'trial' factor since the visual perturbation in AC always occurred at the movement onset. In the FC, we analyzed differences in the spatial error and in the spatial variability with a repeated-measures ANOVA with a single factor session, as only right hand movements were performed.

Post-hoc comparisons were performed using paired sample t-tests. When reported, the nomenclature for the post-hoc comparisons is 'Session-hand' (e.g., Pre-right). Threshold for statistical significance was set at $P < 0.05$ and Bonferroni corrected for multiple comparisons. For all statistical effects involving two or more degrees of freedom, the Greenhouse–Geisser epsilon was used to correct for possible violations of the sphericity assumption (Jennings and Wood, 1976). We report Greenhouse–Geisser epsilon, corrected *P*-values of the ANOVA and the original degrees of freedom.

Diffusion tensor imaging analysis

Based on previous studies where the degree of lateralization of the SLF II (unlike the SLF I and SLF III) has been related to asymmetric performance on visuospatial tasks (Thiebaut de Schotten et al., 2011), a region of interest (ROI) analysis in the SLF II was performed, using a probabilistic SLF II atlas at an 80% probability threshold (kindly provided by M.T. de Schotten).

In order to achieve accurate statistical inference including appropriate correction for multiple comparisons, we used permutation-based non-parametric testing on a voxel-by-voxel basis (Nichols and Holmes, 2002). All normalized and smoothed FA images were entered into a whole brain linear regression analysis using one-sample *t*-test (5000 permutations) and were correlated with the error increase (Post-rTMS error rate–Pre-rTMS error rate) of the right and left hand, respectively. Threshold-free cluster enhancement (Smith and Nichols, 2009) was used to correct results for multiple comparisons using a Family Wise Error (FWE) corrected $P < 0.05$ threshold. Pearson's correlation coefficients were calculated by averaging the FA values across a significant cluster and correlating it with the error increase. The significant clusters were superimposed on the MNI152 template supplied by FSL. FSLview and its atlas tools (International Consortium of Brain Mapping DTI-81 WM label atlas) in addition to general neuroanatomical atlases (Catani et al., 2012) were used to anatomically label the location of significant clusters in MNI152 space.

Results

rTMS-induced deficits in on-line motor control

Fig. 3 compares the error rate in displaced trials for the three sessions and for each hand. The ANOVA showed significant differences in error rate as a function of the session [Session, $F_{2,44} = 16.08$, $P < 0.001$]. A significant session × hand interaction was found [$F_{2,44} = 7.03$, $P < 0.01$, $\varepsilon = 0.76$], showing that differences in error rate depended on the hand that performed the movement. Post-hoc comparisons revealed that the error rate increased after rTMS in both left [Post-left vs. Pre-left, $t_{(22)} = 2.43$, $P < 0.05$] and right [Post-right vs. Pre-right, $t_{(22)} = 4.7$, $P < 0.001$] hand movements. Relative to the Post-rTMS session, a decrease of the error rate was found for the Re-Test session [Post-left vs. Re-Test-left, $t_{(22)} = 5.1$, $P < 0.001$; Post-right vs. Re-Test-right, $t_{(22)} = 5.07$, $P < 0.001$]. The error rate of Pre-rTMS and Re-Test sessions did not differ significantly ($P > 0.37$ in both hands).

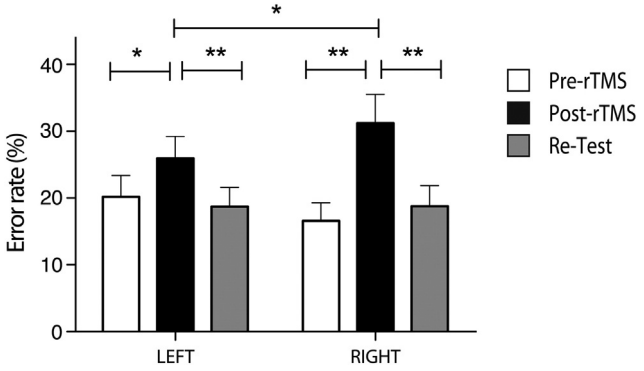

Fig. 3. Behavioral results: bar plot with the mean (±s.e.m.) of the percentage of 'erroneous' responses (non corrective movements when the target jumps) as a function of the session and the hand. *$P < 0.05$; ** $P < 0.01$.

Table 1
Summary of mean values for the error rate (%) in displaced trials of AC and spatial error (mm) in FC. The table reports mean (SD) for each dependent measure.

Adjusting condition						
	Pre-rTMS		Post-rTMS		Re-test	
Error rate (%)	Left 20.2 (15.7)	Right 16.6 (13)	Left 25.6 (15.7)	Right 31.2 (20.9)	Left 18.7 (13.9)	Right 18.9 (14.6)
Fixed condition						
	Pre-rTMS		Post-rTMS		Re-test	
Spatial error (mm)	21.1 (7.8)		20.5 (9.1)		18.9 (8.3)	

Additionally, error rate was higher in the Post-rTMS session for right compared to left hand movements [$t_{(22)} = 2.13$, $P < 0.05$; $P > 0.05$ for all other comparisons]. No significant differences were found between right and left hand in the other two sessions. Error rates are reported in Table 1. Also, the increase of erroneous movements did not correlate neither with the rMT (right hand, $P = 0.26$; left hand, $P = 0.11$) nor with the aMT (right hand, $P = 0.27$; left hand, $P = 0.19$). Fig. 4 illustrates the top view of the hand trajectories of a representative subject. The increase of erroneous trajectories (colored in red) after rTMS is more pronounced for the right hand.

DTI results

The voxel-based analysis revealed a significant negative correlation between the presumed rTMS aftereffect on the right hand's behavior and the FA of the left SLF II (cluster size = 50 voxels, $p_{FWE\text{-}corrected} = 0.03$, peak MNI coordinates = −32, −32, 34). Put simply, the increase of erroneous movements after rTMS application was lower in subjects with higher FA in the contralateral SLF II ($r_{Pearson} = -0.78$) (Fig. 5). No significant clusters were found for the same correlation analysis with the left hand.

Fixed condition

Fig. 6A depicts the hand trajectories of the FC. Here, the trajectory of the hand did not have to be adjusted to target displacement. This condition served as a control to rule out that the impairments seen in the AC could be attributed to unspecific effects of rTMS rather than a specific impairment of the capacity to correct the hand trajectory. The analysis revealed that spatial error was not different across sessions [$F_{2,44} = 1.02$, $P = 0.37$] (Fig. 6B). Also, the dispersion of the hand endpoint position was not affected [$F_{2,44} = 1.54$, $P = 0.23$]. Mean spatial errors are reported in Table 1.

Kinematics

Table 2 compiles the kinematic parameters of AC and FC. Reaction time differed between sessions in the AC [$F_{2,44} = 17.13$, $P < 0.001$, $\varepsilon = 0.72$], being higher in the Pre-rTMS compared to the other sessions ($P < 0.001$) (Fig. 7A). Neither handedness effect ($F_{1,22} = 0.92$, $P = 0.35$) nor a session × hand interaction ($F_{2,44} = 0.46$, $P = 0.63$) were found. We observed a session effect on movement time [$F_{2,44} = 19.93$, $P < 0.001$, $\varepsilon = 0.73$] (Fig. 7B). Post-hoc comparisons revealed slower movements in the Pre-rTMS compared to the other sessions ($P < 0.001$). Movements were longer with the left hand [$F_{1,22} = 4.55$, $P < 0.05$] and in displaced trials [$F_{1,22} = 72.3$, $P < 0.001$]. None of the interactions was significant. The peak velocity was lower in the Pre-rTMS [$F_{2,44} = 10.3$, $P < 0.001$] with respect to either the Post-rTMS ($P < 0.001$) or the Re-Test session ($P < 0.01$), but all other factors and interactions were non-significant. The time to reach the peak velocity in corrective (Fig. 7C) and undisplaced (Fig. 7D) trials revealed a significant effect

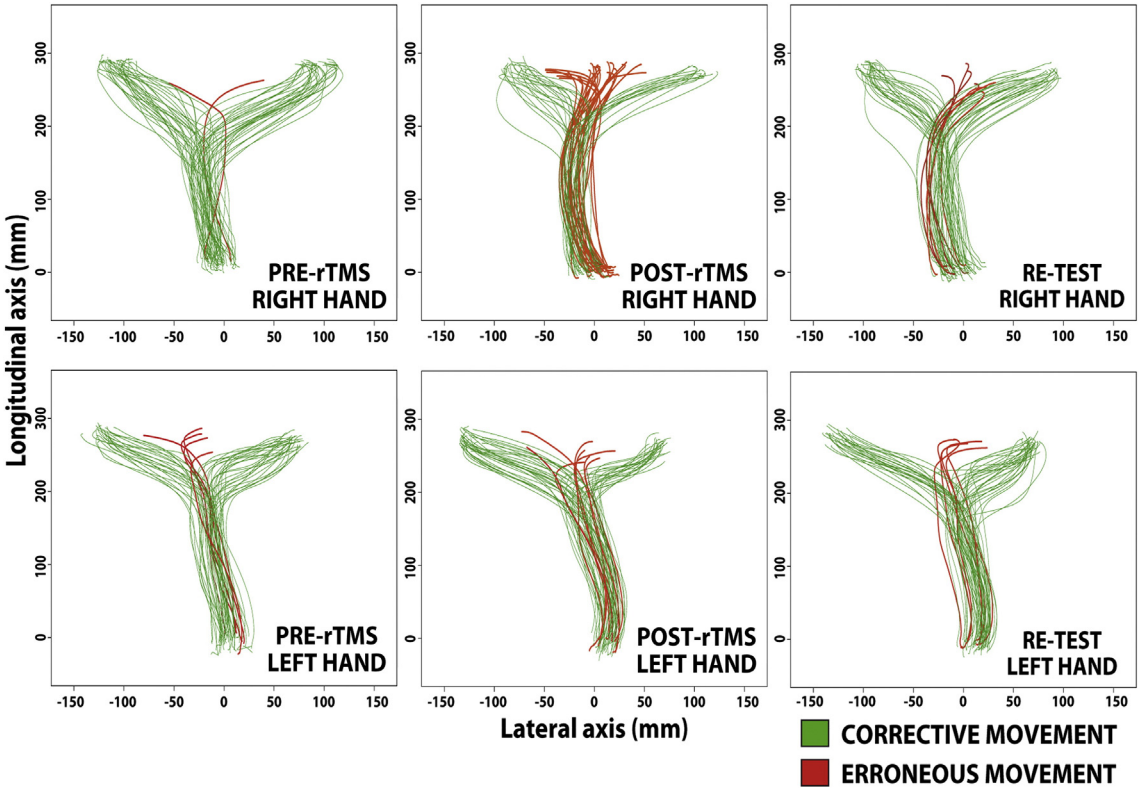

Fig. 4. Top view of the hand trajectories of a representative subject in displaced trials, for each session and for the right (top) and the left (down) hand. Green lines correspond to hand trajectories that were considered as corrective, whereas the red trajectories were non-corrective (erroneous).

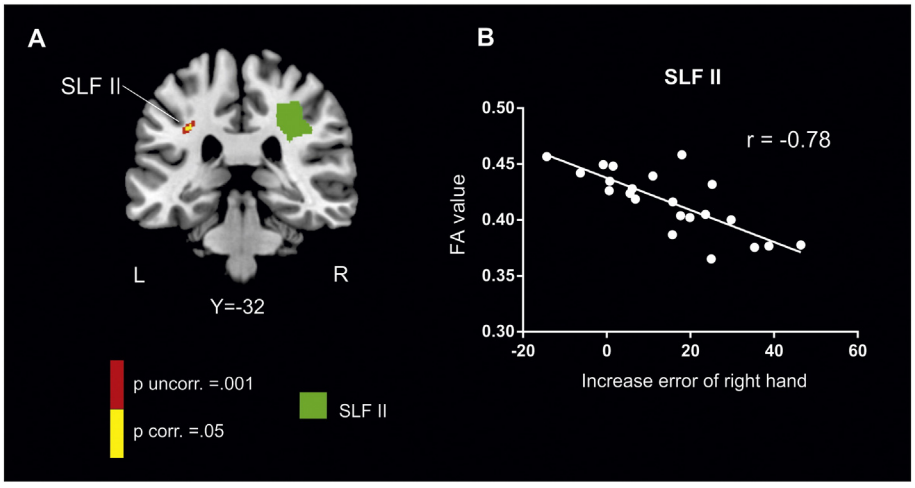

Fig. 5. A. Cluster at contralateral SLF II whose FA values negatively correlated with the error increase of the right hand movements. Maps were thresholded at the $P < 0.05$ FWE corrected level (yellow) and, for visualization purposes, at $P < 0.001$ uncorrected level (red). The cluster is shown over a probabilistic SLF II atlas (green mask) at an 80% probability threshold (obtained from Thiebaut de Schotten et al., 2011). B. Scatter plot showing the negative linear correlation between mean FA values at the left SLF II and the increase of erroneous movements with the right hand immediately after the rTMS protocol. The panel includes the regression line and the correlation coefficient.

of hand [$F_{1,22} = 8.15$, $P < 0.01$], reflecting the fact that right hand movements reached the peak velocity earlier. Deceleration time was different across sessions [$F_{2,44} = 13.4$, $P < 0.001$] and higher for corrective than for undisplaced trials [$F_{1,22} = 69.4$, $P < 0.001$] (Fig. 7E and F). Lastly, the time required to initiate the correction was only modulated as a function of the session [$F_{2,44} = 4.52$, $P = 0.016$], with longer correction times for the slower movements performed in the Pre-rTMS session. Normalized correction time dissipated session effect [$F_{2,44} = 0.04$, $P = 0.96$], but revealed a handedness component [$F_{1,22} = 9.9$, $P < 0.004$] (Fig. 7G and H). None of these kinematic effects was associated with the observed rTMS aftereffects ($p > 0.24$ for all the correlations with the increase of errors). Finally, there was no significant correlation between FA of the left SLF II and none of these kinematic parameters.

In the FC, Pre-rTMS movement times were longer [$F_{2,44} = 9.49$, $P < 0.001$], mainly caused by higher deceleration times [$F_{2,44} = 5.37$, $P = 0.008$]. These movements also showed a lower peak velocity [$F_{2,44} = 3.32$, $P < 0.04$], but the time to reach this velocity was similar across sessions [$F_{2,44} = 1.23$, $P > 0.3$]. Last but not least, the comparison between FC and undisplaced AC trials of the right hand revealed a similar kinematic pattern ($P > 0.07$ for all the comparisons), except for a. higher peak velocity in FC trials [$F_{1,22} = 14.3$, $P < 0.001$].

Discussion

In the present study, we combined rTMS and DTI measures to examine the neurophysiological and anatomical correlates of on-line motor control within the parieto-frontal reaching circuit. As predicted, 15 min of 1-Hz rTMS over the mIPS impaired the ability to correct reaching movements in response to target perturbations, which recovered to baseline values 60 min after the stimulation. DTI analysis revealed that inter-individual differences in the rTMS-induced impairment, measured as the increase of the error rate compared to the Pre-rTMS baseline, were predicted by the individual microstructural properties of the WM fibers in the second branch of the SLF. This tract links the mIPS with prefrontal motor regions that are deeply implicated in action reprogramming. Thus, premotor-parietal WM bundles such as the SLF II may be essential to transmit the on-line computation of motor error when action reprogramming is interfered.

Previous studies have broadly supported the contribution of the mIPS to the on-line control of visually-guided reaching movements (Davare et al., 2012; Desmurget et al., 1999; Grafton et al., 1992). Our data corroborate prior fMRI evidence for an involvement of mIPS in later stages of sensorimotor transformation by coding visual information into a sensorimotor reference (Grefkes et al., 2004; Prado et al., 2005). Previous TMS studies administered a single or a short burst of magnetic pulses in order to momentarily disrupt the mIPS function during specific time intervals (Desmurget et al., 1999; Vesia et al., 2010). 'On-line' TMS indeed is a reliable tool to measure the time-course of the activity of the stimulated area (Amengual et al., 2013; van den Wildenberg et al., 2010). On the other hand, rTMS has demonstrated the induction of local changes in the cortical excitability of the targeted site as well as of remotely connected areas (Fox et al., 1997). As a result, persisting TMS aftereffects can be used to establish a causal relationship between the stimulated brain region, here the mIPS, and its function in a healthy population.

We provide substantial control analyses to rule out other possible confounding variables that could mislead the interpretation of our results. First, all participants performed the task again 60 min after the stimulation (Re-Test session), within a period where the effects of the rTMS were supposed to be completely vanished. This approach has been empirically proven in many prior TMS studies (Chen et al., 1997; Muellbacher et al., 2000; Siebner et al., 1999). We found that the percentage of erroneous responses in the Re-Test session was statistically comparable to those obtained at the baseline measurement. These findings suggest that the increase of errors observed in the Post-rTMS session is not attributable to fatigue effects due to an over-exposition to the task. Secondly, we used an off-line rTMS protocol that allowed participants to perform the task under exactly the same conditions in the three experimental sessions (Pre-rTMS, Post-rTMS and Re-Test). To that end, we used a robotized arm with a motion compensation system that adjusted the coil's position automatically in response to spurious head movements (Amengual et al., 2013; Richter, 2013), increasing the reliability of the outcome after the rTMS application. Thirdly, a remaining issue was whether the increase in error rate after rTMS is due to a more general effect on the motor output rather than a specific effect on movement correction. Koch et al. (2007) modulated the excitability of the primary motor areas by delivering rTMS over other remote but functionally connected areas. Such modulation of activity in primary motor regions should be reflected by changes in kinematic parameters such as movement time and time-to-peak velocity. We analysed a considerable amount of kinematic measures that might explain the increase of erroneous responses when adjusting the movement. In our view, changes in one or more of these parameters as a function of the rTMS would question the specificity of the rTMS effect. However, we found that none of these variables exhibited changes immediately after the rTMS protocol. Although these parameters were slightly shorter for

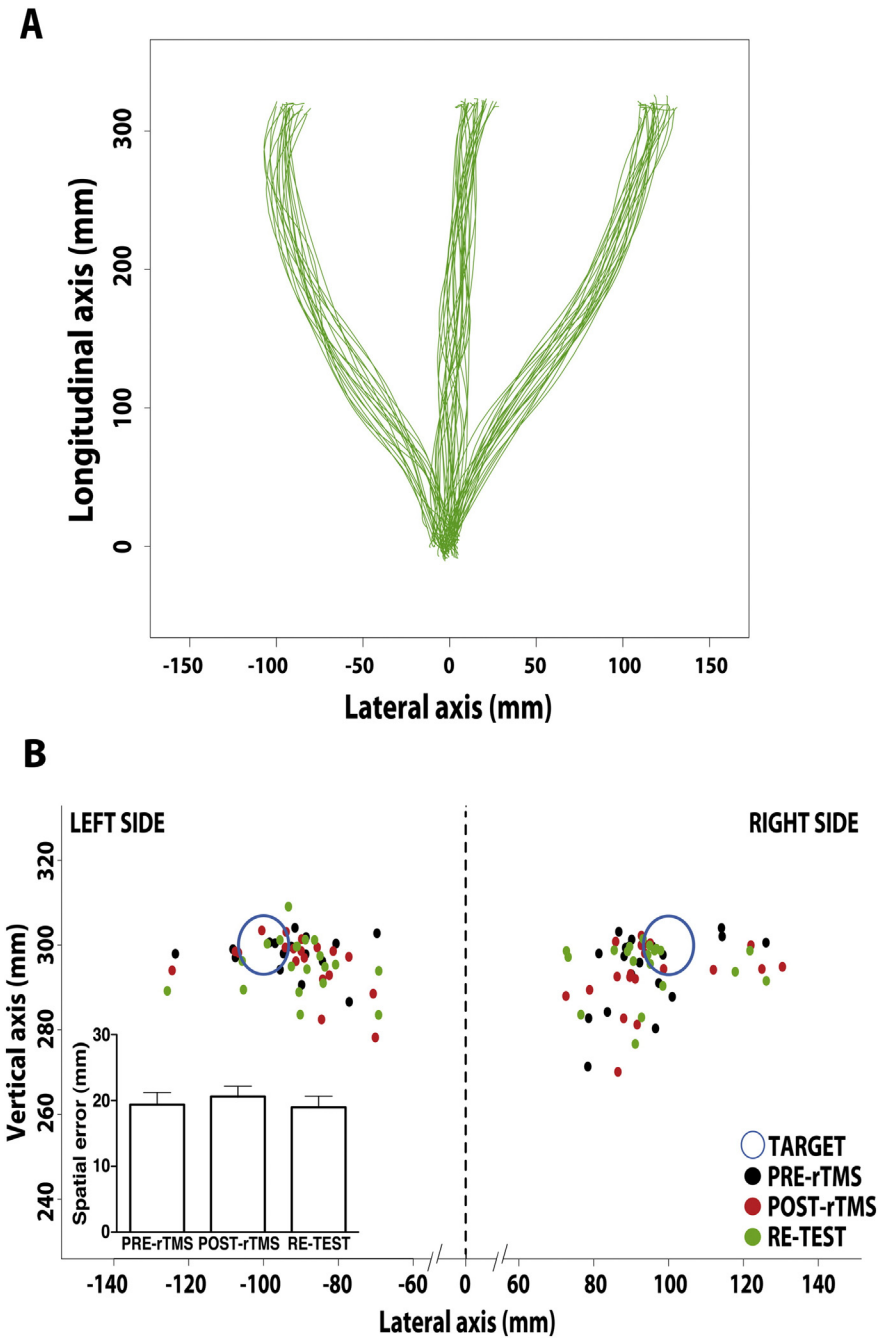

Fig. 6. (A) Top view of the hand trajectories of a representative subject in the FC. (B) 2-D distribution of the spatial error in each side depending on the session. Each dot represents the mean spatial error of one participant in a specific session. Inset: barplot of the mean (±s.e.m.) spatial error committed for each session.

right than for left movements, this effect was present in all sessions and showed no interaction with stimulation, probably reflecting a handedness effect. Reaction times and movement times were longer in the Pre-rTMS session compared to both Post-rTMS and Re-Test, likely reflecting a practice effect (Georgopoulos et al., 1981). None of these training effects were thus associated with the observed behavioral rTMS aftereffects. Altogether, these evidences suggest that the increase of errors in the Post-rTMS session is due to the stimulation of the mIPS, rather than due to a global effect on the motor output.

The behavioral counterpart of the application of the rTMS over the left mIPS predominantly influenced contralateral (right) hand movements. Smaller but significant effects were also observed for ipsilateral hand movements. Conflicting data has been reported regarding the hemispheric specificity of on-line adjustments (Desmurget et al., 1999; Vesia et al., 2010). Our results concur with imaging studies showing bilateral fronto-parietal activations with contralateral predominance (Medendorp et al., 2003). Noteworthy, movements with the non-dominant hand showed higher error rates than those performed with the dominant hand during the Pre-rTMS session. This is consistent with previous studies reporting manual asymmetries and a superior ability of the dominant hemisphere to correct movements (Boulinguez et al., 2001; Sainburg and Kalakanis, 2000). Importantly, the lack of differences in the FC shows that the target location was processed properly after rTMS, and thus our effects cannot be explained by an rTMS-induced impairment of visual processes. Hence, the increase of the error rate in later stages of sensorimotor integration appears to reflect genuine effects of inhibition of the mIPS (Davare et al., 2012).

Table 2
Summary of kinematic parameters in AC (undisplaced and corrective trials) and in FC. The table reports mean (SD). RT: reaction time; MT: movement time; PV: peak velocity; TPV: time to peak velocity; DT: deceleration time; CT: correction time.

Adjusting condition

	Pre-rTMS		Post-rTMS		Re-test	
RT (ms)	Left	Right	Left	Right	Left	Right
	259 (28)	259 (22)	248 (23)	250 (24)	244 (21)	247 (17)

Adjusting condition — undisplaced trials

	Pre-rTMS		Post-rTMS		Re-test	
MT (ms)	Left	Right	Left	Right	Left	Right
	357 (48)	352 (45)	330 (49)	315 (50)	335 (54)	325 (55)
PV (mm/s)	Left	Right	Left	Right	Left	Right
	2648 (573)	2652 (587)	2929 (651)	2992 (663)	2851 (656)	2851 (751)
TPV (ms)	Left	Right	Left	Right	Left	Right
	163 (25)	150 (29)	155 (29)	143 (29)	159 (32)	150 (30)
DT (ms)	Left	Right	Left	Right	Left	Right
	194 (48)	202 (63)	175 (55)	171 (66)	176 (59)	175 (66)

Adjusting condition — corrective trials

	Pre-rTMS		Post-rTMS		Re-test	
MT (ms)	Left	Right	Left	Right	Left	Right
	397 (55)	391 (46)	376 (58)	362 (60)	377 (65)	369 (62)
PV (mm/s)	Left	Right	Left	Right	Left	Right
	2594 (596)	2654 (564)	2896 (612)	2910 (658)	2931 (703)	2797 (699)
TPV (ms)	Left	Right	Left	Right	Left	Right
	162 (26)	147 (26)	155 (28)	142 (29)	161 (30)	149 (30)
DT (ms)	Left	Right	Left	Right	Left	Right
	235 (61)	244 (63)	220 (69)	220 (74)	215 (71)	220 (73)
CT (ms)	Left	Right	Left	Right	Left	Right
	215 (38)	198 (27)	192 (32)	190 (31)	199 (36)	185 (30)

Fixed condition

	Pre-rTMS	Post-rTMS	Re-test
RT (ms)	257 (22)	252 (22)	250 (21)
MT (ms)	343 (44)	315 (42)	319 (51)
PV (mm/s)	2991 (632)	3193 (727)	3127 (736)
TPV (ms)	160 (36)	151 (39)	157 (32)
DT (ms)	183 (58)	164 (52)	162 (53)

The elucidation of the nature and extent of inter-subject variation is critical for understanding the neural basis of on-line motor control in normal and abnormal populations. Important individual differences have been found in healthy adults performing goal-directed reaching that required on-line adjustments of the movement to unexpected visual perturbations (Boy et al., 2010; Reichenbach et al., 2008). In the present study, we also found considerable inter-individual differences in the ability to perform on-line adjustments of movements after rTMS intervention, echoing results from previous studies (Desmurget et al., 1999). Many factors can contribute to this variability in rTMS aftereffects, including gender, time of day, age and neuromodulators (see Ridding and Ziemann, 2010 for review). Specifically, some studies have suggested that the thickness of the stimulated cortex and the interneurons recruited by the TMS pulse might be pivotal neuroanatomical predictors of the expected rTMS effect (Conde et al., 2012; Hamada et al., 2013; Ziemann and Siebner, 2015). In our study, we addressed how the inter-subject variability of the rTMS aftereffects could be determined by the microstructural features of the WM pathways interconnecting the targeted and other networked brain areas. To that end, we calculated the correlation between the increase of the error rate produced by the rTMS and the FA as an index of the microstructural properties of the WM tract. This analysis showed that participants with stronger contralateral behavioral consequences after rTMS application (that is, a greater reduction of on-line corrections with the right hand) exhibited higher FA values in the contralateral SLF II. The SLF II transmits information within the premotor-parietal network that connects the IPS and the PMd (Boorman et al., 2007; Thiebaut de Schotten et al., 2012). The reported cortico-cortical parieto-frontal pathway between the medial bank of the IPS and PMd in monkeys (Johnson and Ferraina, 1996; Wise et al., 1997) has found an homologue circuit in humans, emphasizing the concomitant contribution of dorsal premotor areas and the mIPS (Chouinard et al., 2003) and stating the importance of PMd in action reprogramming (Hartwigsen et al., 2012). In general, the PMd is held to be required when a new motor plan is initiated or its goal changed in a discrete/intermittent fashion (Archambault et al., 2009). Therefore, rTMS over the mIPS might modulate its inputs into the rostral PMd (Caminiti et al., 1996), affecting its capacity to reprogram the movement towards the new location of the target. Our results therefore suggest that the SLF II might have an active role in mediating the dynamic computation of the motor error from the mIPS to the PMd.

It is noteworthy that the sign of the correlation indicates that the behavioral after effects of the rTMS were weaker in subjects showing higher FA. This finding is consistent with prior studies that reported a negative relationship between the TMS-induced modulation of visual sensitivity and the fronto-tectal WM connectivity (Quentin et al., 2013, 2014). Considering the 'virtual-lesion' model, in which inhibitory rTMS might act as a breakdown of the function associated to the targeted area, these results are also in line with previous clinical studies in traumatic brain injury (TBI) (Strangman et al., 2012) and stroke patients (Qiu et al., 2011). In these studies, FA predicts their prognosis, that is to say, FA is considered as a biomarker that might anticipate which of these patients will recover their functional deficit and which not. Inhibitory rTMS over the mIPS causes a virtual partial lesion decreasing the excitability in this area. The efficacy with which a TMS-modulated node of the premotor-parietal network (in this case the mIPS) affects other remote nodes in the same network, might be partially determined by the structural substrate of premotor-parietal connections, such as the SLF II.

This study presents some limitations or caveats that deserve further discussion. Although we have strong arguments supporting that the application of the rTMS on the mIPS induced specific decrease of corrective trajectories, our experimental approach do not completely exclude the possibility that this effects were due to non-specific observations. In this context, the inclusion of a proper control condition such as the stimulation of another region within or without the parieto-frontal network, or even a sham condition with non-real stimulation would shed more light on the specific relationship between the stimulated area and the behavioral counterpart. Another limitation is that our work is indeed blind to the physiological mechanisms underlying the present findings. In addition to local changes in the cortical excitability of the target site, it is known that rTMS also influences the excitability of remotely connected areas (Fox et al., 2012). Therefore, the microstructural properties of the WM tracts linking these regions might modulate the extent of these changes. FA is an index of deviation or directionality of water diffusion from a random spherical displacement and is thought to reflect factors such as axonal injury and demyelination that are important for understanding neurological disease (Kloppel et al., 2008; Stinear et al., 2007; Strangman et al., 2012). This is deeply rooted in the concept that the anisotropy of water diffusion can probe microscopic details about the anatomical architecture of neural tissues, which is likely influenced by a number of factors, including the degree of myelination, the density, diameter distribution, and orientational coherence of axons (Beaulieu, 2002). Importantly, while FA is highly sensitive to microstructural changes, it is less specific to the

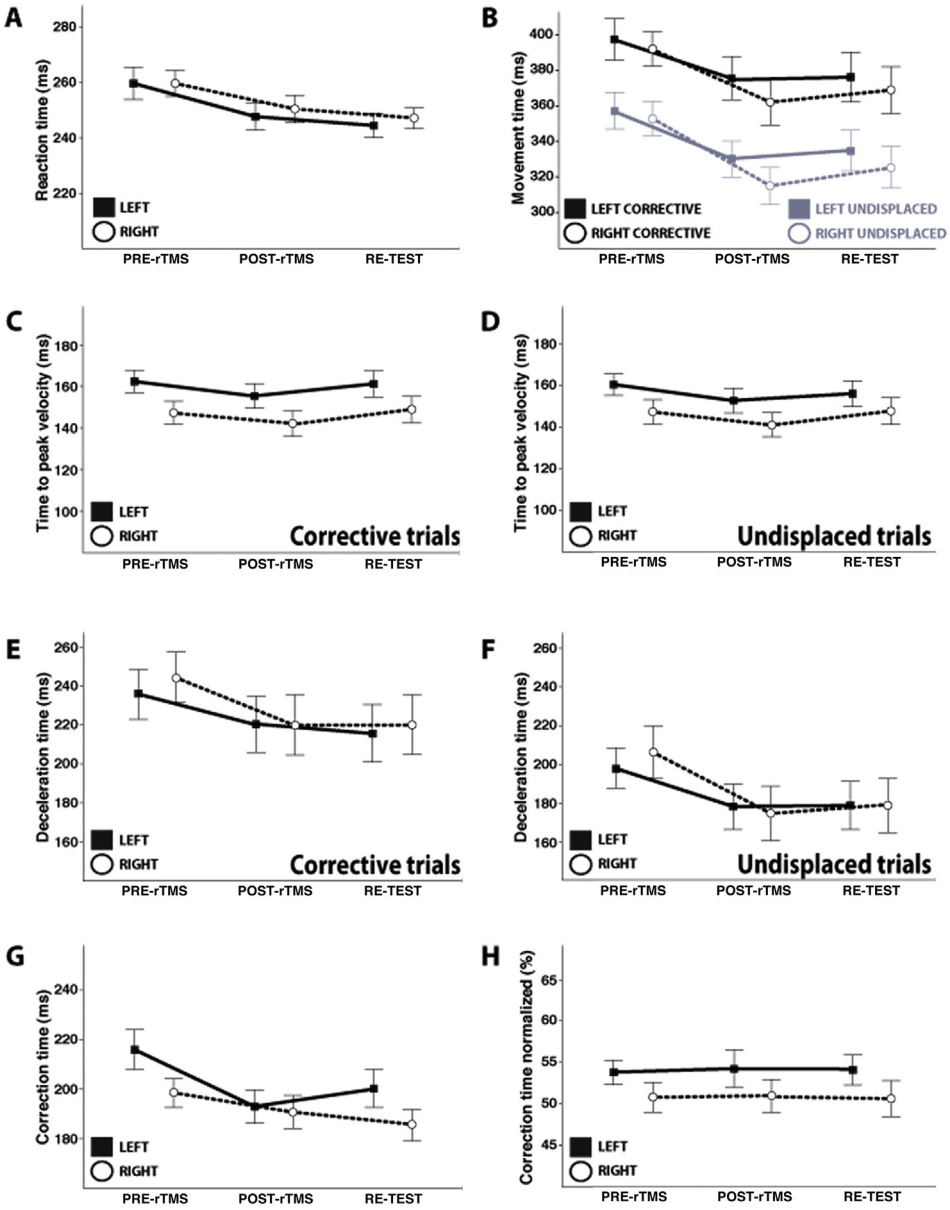

Fig. 7. Mean (±s.e.m.) for the kinematics of the AC. Right and left hand conditions are indicated by white circle and black square, respectively. (A) Differences in reaction time splitted by session and hand, including all trials of the AC. B. Movement time for each session and hand comparing undisplaced (gray) and corrective (black) trials. Time-to-peak velocity values for corrective (C) and undisplaced (D) trials. Deceleration time for corrective (E) and undisplaced (F) trials. G. Differences in the time needed to initiate an on-line correction, for each session and hand. H. Correction time normalized with respect to movement time.

type of change (e.g., axial or radial). Tentatively, one possibility is that the observed correlation between FA and rTMS effect could be associated to the influence of myelin thickness on both water self-diffusion and nerve conduction velocity (Jack et al., 1983). However, increased FA values could also be associated to a more densely packed tract or to a higher number of axons of mIPS neurons projecting to the PMd. Independently of the underlying mechanism responsible for the increased FA, it would predict a faster and more efficient conduction velocity which would in turn result in a faster and more precise action reprogramming. More evidence will be required, however, to make strong claims about the underlying physiological mechanism that links the motor impairment caused by the rTMS and the anatomical correlates of the 'reaching' circuit.

In conclusion, a 15-min period of inhibitory rTMS (1 Hz) of the left mIPS produced an impairment of the ability to adaptively control motor responses immediately after the stimulation. The degree of this impairment was related to the microstructural properties of the SLF II, the tract that connects the targeted region and the PMd. We believe that these results have important implications to establish DTI-derived surrogate markers of motor impairment and to our understanding of the structural/functional correlates that subserve on-line motor control.

Acknowledgments

We acknowledge Pablo Ripollés for his contribution and advice on DTI analysis, and Michel Thiebaut de Schotten for providing the probabilistic SLF atlas. We are very grateful to Katrin Sellin for his valuable help during the execution of the study. This work was supported by an AGAUR B.E. grant from the Catalan government (BE-DGR 2011) to BRH and JLA, a Spanish government grant to ARF (PSI2012-29219) and a grant from the Generalitat de Catalunya (SGR2005-00831). TFM is supported by the DFG (SFB TR134 C1) and the BMBF (01GJ1009).

Competing interests

The authors declare no disclosure of financial interests and potential conflict of interest.

References

Amengual, J.L., Marco-Pallares, J., Richter, L., Oung, S., Schweikard, A., Mohammadi, B., Rodriguez-Fornells, A., Munte, T.F., 2013. Tracking post-error adaptation in the motor system by transcranial magnetic stimulation. Neuroscience 250, 342–351.

Andersen, R.A., Buneo, C.A., 2002. Intentional maps in posterior parietal cortex. Annu. Rev. Neurosci. 25, 189–220.

Andersen, R.A., Snyder, L.H., Bradley, D.C., Xing, J., 1997. Multimodal representation of space in the posterior parietal cortex and its use in planning movements. Annu. Rev. Neurosci. 20, 303–330.

Andersson, J.L., Jenkinson, M., Smith, S., 2007a. Non-linear Optimisation FMRIB Technical Report TR07JA1. University of Oxford FMRIB Centre, Oxford.

Andersson, J.L., Jenkinson, M., Smith, S., 2007b. Non-linear Registration, Aka Spatial Normalisation FMRIB Technical Report TR07JA2. FMRIB Analysis Group of the University of Oxford.

Archambault, P.S., Caminiti, R., Battaglia-Mayer, A., 2009. Cortical mechanisms for online control of hand movement trajectory: the role of the posterior parietal cortex. Cereb. Cortex 19, 2848–2864.

Beaulieu, C., 2002. The basis of anisotropic water diffusion in the nervous system—a technical review. NMR Biomed. 15, 435–455.

Behrens, T.E., Johansen-Berg, H., 2005. Relating connectional architecture to grey matter function using diffusion imaging. Philos. Trans. R. Soc. Lond. Ser. B Biol. Sci. 360, 903–911.

Blangero, A., Menz, M.M., McNamara, A., Binkofski, F., 2009. Parietal modules for reaching. Neuropsychologia 47, 1500–1507.

Boorman, E.D., O'Shea, J., Sebastian, C., Rushworth, M.F., Johansen-Berg, H., 2007. Individual differences in white-matter microstructure reflect variation in functional connectivity during choice. Curr. Biol. 17, 1426–1431.

Boulinguez, P., Nougier, V., Velay, J.L., 2001. Manual asymmetries in reaching movement control. I: Study of right-handers. Cortex 37, 101–122.

Boy, F., Evans, C.J., Edden, R.A., Singh, K.D., Husain, M., Sumner, P., 2010. Individual differences in subconscious motor control predicted by GABA concentration in SMA. Curr. Biol. 20, 1779–1785.

Buelte, D., Meister, I.G., Staedtgen, M., Dambeck, N., Sparing, R., Grefkes, C., Boroojerdi, B., 2008. The role of the anterior intraparietal sulcus in crossmodal processing of object features in humans: an rTMS study. Brain Res. 1217, 110–118.

Càmara, E., Bodammer, N., Rodríguez-Fornells, A., Tempelmann, C., 2007. Age-related water diffusion changes in human brain: a voxel-based approach. Neuroimage 34, 1588–1599.

Caminiti, R., Ferraina, S., Johnson, P.B., 1996. The sources of visual information to the primate frontal lobe: a novel role for the superior parietal lobule. Cereb. Cortex 6, 319–328.

Catani, M., de Schotten, M.T., 2012. Atlas of human brain connections: Oxford University Press.

Chen, R., Classen, J., Gerloff, C., Celnik, P., Wassermann, E.M., Hallett, M., Cohen, L.G., 1997. Depression of motor cortex excitability by low-frequency transcranial magnetic stimulation. Neurology 48, 1398–1403.

Chouinard, P.A., Van Der Werf, Y.D., Leonard, G., Paus, T., 2003. Modulating neural networks with transcranial magnetic stimulation applied over the dorsal premotor and primary motor cortices. J. Neurophysiol. 90, 1071–1083.

Clower, D.M., Hoffman, J.M., Votaw, J.R., Faber, T.L., Woods, R.P., Alexander, G.E., 1996. Role of posterior parietal cortex in the recalibration of visually guided reaching. Nature 383, 618–621.

Colebatch, J.G., Deiber, M.P., Passingham, R.E., Friston, K.J., Frackowiak, R.S., 1991. Regional cerebral blood flow during voluntary arm and hand movements in human subjects. J. Neurophysiol. 65, 1392–1401.

Conde, V., Vollmann, H., Sehm, B., Taubert, M., Villringer, A., Ragert, P., 2012. Cortical thickness in primary sensorimotor cortex influences the effectiveness of paired associative stimulation. Neuroimage 60, 864–870.

Culham, J.C., Danckert, S.L., DeSouza, J.F., Gati, J.S., Menon, R.S., Goodale, M.A., 2003. Visually guided grasping produces fMRI activation in dorsal but not ventral stream brain areas. Exp. Brain Res. 153, 180–189.

Darquie, A., Poline, J.B., Poupon, C., Saint-Jalmes, H., Le Bihan, D., 2001. Transient decrease in water diffusion observed in human occipital cortex during visual stimulation. Proc. Natl. Acad. Sci. U. S. A. 98, 9391–9395.

Davare, M., Zenon, A., Pourtois, G., Desmurget, M., Olivier, E., 2012. Role of the medial part of the intraparietal sulcus in implementing movement direction. Cereb. Cortex 22, 1382–1394.

Della-Maggiore, V., Malfait, N., Ostry, D.J., Paus, T., 2004. Stimulation of the posterior parietal cortex interferes with arm trajectory adjustments during the learning of new dynamics. J. Neurosci. 24, 9971–9976.

Desmurget, M., Epstein, C.M., Turner, R.S., Prablanc, C., Alexander, G.E., Grafton, S.T., 1999. Role of the posterior parietal cortex in updating reaching movements to a visual target. Nat. Neurosci. 2, 563–567.

Desmurget, M., Grea, H., Grethe, J.S., Prablanc, C., Alexander, G.E., Grafton, S.T., 2001. Functional anatomy of nonvisual feedback loops during reaching: a positron emission tomography study. J. Neurosci. 21, 2919–2928.

Fox, P., Ingham, R., George, M.S., Mayberg, H., Ingham, J., Roby, J., Martin, C., Jerabek, P., 1997. Imaging human intra-cerebral connectivity by PET during TMS. Neuroreport 8, 2787–2791.

Fox, M.D., Halko, M.A., Eldaief, M.C., Pascual-Leone, A., 2012. Measuring and manipulating brain connectivity with resting state functional connectivity magnetic resonance imaging (fcMRI) and transcranial magnetic stimulation (TMS). Neuroimage 62, 2232–2243.

Frey, S.H., Vinton, D., Norlund, R., Grafton, S.T., 2005. Cortical topography of human anterior intraparietal cortex active during visually guided grasping. Brain Res. Cogn. Brain Res. 23, 397–405.

Fuentemilla, Ll, Càmara, E., Münte, T.F., Krämer, U., Cunillera, T., Marco-Pallarés, J., Tempelmann, C., Rodríguez-Fornells, A., 2009. Individual differences in true and false memory retrieval are related to white matter brain microstructure. J. Neurosci. 29, 8698–8703.

Georgopoulos, A.P., Kalaska, J.F., Massey, J.T., 1981. Spatial trajectories and reaction times of aimed movements: effects of practice, uncertainty, and change in target location. J. Neurophysiol. 46, 725–743.

Gerschlager, W., Siebner, H.R., Rothwell, J.C., 2001. Decreased corticospinal excitability after subthreshold 1 Hz rTMS over lateral premotor cortex. Neurology 57, 449–455.

Glover, S., Miall, R.C., Rushworth, M.F., 2005. Parietal rTMS disrupts the initiation but not the execution of on-line adjustments to a perturbation of object size. J. Cogn. Neurosci. 17, 124–136.

Grafton, S.T., Mazziotta, J.C., Presty, S., Friston, K.J., Frackowiak, R.S., Phelps, M.E., 1992. Functional anatomy of human procedural learning determined with regional cerebral blood flow and PET. J. Neurosci. 12, 2542–2548.

Granek, J.A., Pisella, L., Blangero, A., Rossetti, Y., Sergio, L.E., 2012. The role of the caudal superior parietal lobule in updating hand location in peripheral vision: further evidence from optic ataxia. PLoS One 7 e46619.

Grefkes, C., Ritzl, A., Zilles, K., Fink, G.R., 2004. Human medial intraparietal cortex subserves visuomotor coordinate transformation. Neuroimage 23, 1494–1506.

Hamada, M., Murase, N., Hasan, A., Balaratnam, M., Rothwell, J.C., 2013. The role of interneuron networks in driving human motor cortical plasticity. Cereb. Cortex 23, 1593–1605.

Hartwigsen, G., Bestmann, S., Ward, N.S., Woerbel, S., Mastroeni, C., Granert, O., Siebner, H.R., 2012. Left dorsal premotor cortex and supramarginal gyrus complement each other during rapid action reprogramming. J. Neurosci. 32, 16162–16171a.

Huang, Y.Z., Edwards, M.J., Rounis, E., Bhatia, K.P., Rothwell, J.C., 2005. Theta burst stimulation of the human motor cortex. Neuron 45, 201–206.

Jack, J.J.B., Noble, D., Tsien, R.W., 1983. Electric Current Flow in Excitable Cells. Oxford University Press, New York.

Jennings, J.R., Wood, C.C., 1976. Letter: the epsilon-adjustment procedure for repeated-measures analyses of variance. Psychophysiology 13, 277–278.

Johnson, P.B., Ferraina, S., 1996. Cortical networks for visual reaching: intrinsic frontal lobe connectivity. Eur. J. Neurosci. 8, 1358–1362.

Johnson, P.B., Ferraina, S., Caminiti, R., 1993. Cortical networks for visual reaching. Exp. Brain Res. 97, 361–365.

Kertzman, C., Schwarz, U., Zeffiro, T.A., Hallett, M., 1997. The role of posterior parietal cortex in visually guided reaching movements in humans. Exp. Brain Res. 114, 170–183.

Kimiwada, T., Juhasz, C., Makki, M., Muzik, O., Chugani, D.C., Asano, E., Chugani, H.T., 2006. Hippocampal and thalamic diffusion abnormalities in children with temporal lobe epilepsy. Epilepsia 47, 167–175.

Kloppel, S., Baumer, T., Kroeger, J., Koch, M.A., Buchel, C., Munchau, A., Siebner, H.R., 2008. The cortical motor threshold reflects microstructural properties of cerebral white matter. Neuroimage 40, 1782–1791.

Koch, G., Oliveri, M., Torriero, S., Salerno, S., Lo Gerfo, E., Caltagirone, C., 2007. Repetitive TMS of cerebellum interferes with millisecond time processing. Exp. Brain Res. 179, 291–299.

Le Bihan, D., Urayama, S., Aso, T., Hanakawa, T., Fukuyama, H., 2006. Direct and fast detection of neuronal activation in the human brain with diffusion MRI. Proc. Natl. Acad. Sci. U. S. A. 103, 8263–8268.

Liu, G., McMillan, L., 2006. Estimation of missing markers in human motion capture. Vis. Comput. 22, 721–728.

Machii, K., Cohen, D., Ramos-Estebanez, C., Pascual-Leone, A., 2006. Safety of rTMS to non-motor cortical areas in healthy participants and patients. Clin. Neurophysiol. 117, 455–471.

Makris, N., Kennedy, D.N., McInerney, S., Sorensen, A.G., Wang, R., Caviness Jr., V.S., Pandya, D.N., 2005. Segmentation of subcomponents within the superior longitudinal fascicle in humans: a quantitative, in vivo, DT-MRI study. Cereb. Cortex 15, 854–869.

Mason, C.R., Gomez, J.E., Ebner, T.J., 2001. Hand synergies during reach-to-grasp. J. Neurophysiol. 86, 2896–2910.

Matthaus, L., 2008. A robotic assistance system for transcranial magnetic stimulation and its application to motor cortex mapping. Institute for Robotics and Cognitive Systems. University of Lübeck, p. 166.

Medendorp, W.P., Goltz, H.C., Vilis, T., Crawford, J.D., 2003. Gaze-centered updating of visual space in human parietal cortex. J. Neurosci. 23, 6209–6214.

Messier, J., Kalaska, J.F., 1999. Comparison of variability of initial kinematics and endpoints of reaching movements. Exp. Brain Res. 125, 139–152.

Muellbacher, W., Ziemann, U., Boroojerdi, B., Hallett, M., 2000. Effects of low-frequency transcranial magnetic stimulation on motor excitability and basic motor behavior. Clin. Neurophysiol. 111, 1002–1007.

Neggers, S.F., Bekkering, H., 2002. Coordinated control of eye and hand movements in dynamic reaching. Hum. Mov. Sci. 21, 349–376.

Nichols, T.E., Holmes, A.P., 2002. Nonparametric permutation tests for functional neuroimaging: A primer with examples. Hum. Brain Mapp. 15, 1–25.

Oldfield, R.C., 1971. The assessment and analysis of handedness: the Edinburgh inventory. Neuropsychologia 9, 97–113.

Petrides, M., Pandya, D.N., 1984. Projections to the frontal cortex from the posterior parietal region in the rhesus monkey. J. Comp. Neurol. 228, 105–116.
Pisella, L., Grea, H., Tilikete, C., Vighetto, A., Desmurget, M., Rode, G., Boisson, D., Rossetti, Y., 2000. An 'automatic pilot' for the hand in human posterior parietal cortex: toward reinterpreting optic ataxia. Nat. Neurosci. 3, 729–736.
Prado, J., Clavagnier, S., Otzenberger, H., Scheiber, C., Kennedy, H., Perenin, M.T., 2005. Two cortical systems for reaching in central and peripheral vision. Neuron 48, 849–858.
Qiu, M., Darling, W.G., Morecraft, R.J., Ni, C.C., Rajendra, J., Butler, A.J., 2011. White matter integrity is a stronger predictor of motor function than BOLD response in patients with stroke. Neurorehabil. Neural Repair 25, 275–284.
Quentin, R., Chanes, L., Migliaccio, R., Valabregue, R., Valero-Cabre, A., 2013. Fronto-tectal white matter connectivity mediates facilitatory effects of non-invasive neurostimulation on visual detection. Neuroimage 82, 344–354.
Quentin, R., Chanes, L., Vernet, M., Valero-Cabre, A., 2014. Fronto-parietal anatomical connections influence the modulation of conscious visual perception by high-beta frontal oscillatory activity. Cereb. Cortex 25, 2095–2101.
Reichenbach, A., Bresciani, J.-P., Peer, A., Bülthoff, H., Thielscher, A., 2008. Inter-individual spatial diversity in motor control processes within the posterior parietal cortex assessed with transcranial magnetic stimulation. Brain Stimul. 1, 283–284.
Rey, M., Dellatolas, G., Bancaud, J., Talairach, J., 1988. Hemispheric lateralization of motor and speech functions after early brain lesion: study of 73 epileptic patients with intracarotid amytal test. Neuropsychologia 26, 167–172.
Richter, L., 2013. Robotized Transcranial Magnetic Stimulation. 1st ed. Springer New York, New York.
Richter, L., Ernst, F., Schlaefer, A., Schweikard, A., 2011. Robust real-time robot-world calibration for robotized transcranial magnetic stimulation. Int. J. Med. Rob. Comput. Assisted Surg. 7, 414–422.
Richter, L., Trillenberg, P., Schweikard, A., Schlaefer, A., 2013. Stimulus intensity for hand held and robotic transcranial magnetic stimulation. Brain Stimul. 6, 315–321.
Ridding, M.C., Ziemann, U., 2010. Determinants of the induction of cortical plasticity by non-invasive brain stimulation in healthy subjects. J. Physiol. 588, 2291–2304.
Rodriguez-Herreros, B., Lopez-Moliner, J., 2011. Proprioception improves temporal accuracy in a coincidence-timing task. Exp. Brain Res. 210, 251–258.
Rossini, P.M., Barker, A.T., Berardelli, A., Caramia, M.D., Caruso, G., Cracco, R.Q., Dimitrijevic, M.R., Hallett, M., Katayama, Y., Lucking, C.H., et al., 1994. Non-invasive electrical and magnetic stimulation of the brain, spinal cord and roots: basic principles and procedures for routine clinical application. Report of an IFCN committee. Electroencephalogr. Clin. Neurophysiol. 91, 79–92.
Sainburg, R.L., Kalakanis, D., 2000. Differences in control of limb dynamics during dominant and nondominant arm reaching. J. Neurophysiol. 83, 2661–2675.
Sakata, H., Taira, M., Murata, A., Mine, S., 1995. Neural mechanisms of visual guidance of hand action in the parietal cortex of the monkey. Cereb. Cortex 5, 429–438.
Schmahmann, J.D., Pandya, D.N., 2006. Fiber Pathways of the Brain. Oxford University Press, Oxford; New York.
Schmahmann, J.D., Pandya, D.N., Wang, R., Dai, G., D'Arceuil, H.E., de Crespigny, A.J., Wedeen, V.J., 2007. Association fibre pathways of the brain: parallel observations from diffusion spectrum imaging and autoradiography. Brain 130, 630–653.
Siebner, H.R., Mentschel, C., Auer, C., Conrad, B., 1999. Repetitive transcranial magnetic stimulation has a beneficial effect on bradykinesia in Parkinson's disease. Neuroreport 10, 589–594.
Siebner, H.R., Peller, M., Willoch, F., Minoshima, S., Boecker, H., Auer, C., Drzezga, A., Conrad, B., Bartenstein, P., 2000. Lasting cortical activation after repetitive TMS of the motor cortex: a glucose metabolic study. Neurology 54, 956–963.
Siebner, H.R., Hartwigsen, G., Kassuba, T., Rothwell, J.C., 2009. How does transcranial magnetic stimulation modify neuronal activity in the brain? Implications for studies of cognition. Cortex 45, 1035–1042.
Smith, S.M., Nichols, T.E., 2009. Threshold-free cluster enhancement: addressing problems of smoothing, threshold dependence and localisation in cluster inference. Neuroimage 44, 83–98.
Smith, S.M., Zhang, Y., Jenkinson, M., Chen, J., Matthews, P.M., Federico, A., De Stefano, N., 2002. Accurate, robust, and automated longitudinal and cross-sectional brain change analysis. Neuroimage 17, 479–489.
Smith, S.M., Jenkinson, M., Woolrich, M.W., Beckmann, C.F., Behrens, T.E., Johansen-Berg, H., Bannister, P.R., De Luca, M., Drobnjak, I., Flitney, D.E., Niazy, R.K., Saunders, J., Vickers, J., Zhang, Y., De Stefano, N., Brady, J.M., Matthews, P.M., 2004. Advances in functional and structural MR image analysis and implementation as FSL. Neuroimage 23 (Suppl. 1), S208–S219.
Steinman, R.M., Kowler, E., Collewijn, H., 1990. New directions for oculomotor research. Vis. Res. 30, 1845–1864.
Stinear, C.M., Barber, P.A., Smale, P.R., Coxon, J.P., Fleming, M.K., Byblow, W.D., 2007. Functional potential in chronic stroke patients depends on corticospinal tract integrity. Brain 130, 170–180.
Strangman, G.E., O'Neil-Pirozzi, T.M., Supelana, C., Goldstein, R., Katz, D.I., Glenn, M.B., 2012. Fractional anisotropy helps predicts memory rehabilitation outcome after traumatic brain injury. NeuroRehabilitation 31, 295–310.
Thiebaut de Schotten, M., Dell'Acqua, F., Forkel, S.J., Simmons, A., Vergani, F., Murphy, D.G., Catani, M., 2011. A lateralized brain network for visuospatial attention. Nat. Neurosci. 14, 1245–1246.
Thiebaut de Schotten, M., Dell'Acqua, F., Valabregue, R., Catani, M., 2012. Monkey to human comparative anatomy of the frontal lobe association tracts. Cortex 48, 82–96.
Tunik, E., Frey, S.H., Grafton, S.T., 2005. Virtual lesions of the anterior intraparietal area disrupt goal-dependent on-line adjustments of grasp. Nat. Neurosci. 8, 505–511.
Tunik, E., Rice, N.J., Hamilton, A., Grafton, S.T., 2007. Beyond grasping: representation of action in human anterior intraparietal sulcus. Neuroimage 36 (Suppl. 2), T77–T86.
van Beers, R.J., Haggard, P., Wolpert, D.M., 2004. The role of execution noise in movement variability. J. Neurophysiol. 91, 1050–1063.
van den Wildenberg, W.P., Burle, B., Vidal, F., van der Molen, M.W., Ridderinkhof, K.R., Hasbroucq, T., 2010. Mechanisms and dynamics of cortical motor inhibition in the stop-signal paradigm: a TMS study. J. Cogn. Neurosci. 22, 225–239.
Vesia, M., Prime, S.L., Yan, X., Sergio, L.E., Crawford, J.D., 2010. Specificity of human parietal saccade and reach regions during transcranial magnetic stimulation. J. Neurosci. 30, 13053–13065.
Wassermann, E.M., Wedegaertner, F.R., Ziemann, U., George, M.S., Chen, R., 1998. Crossed reduction of human motor cortex excitability by 1-Hz transcranial magnetic stimulation. Neurosci. Lett. 250, 141–144.
Wise, S.P., Boussaoud, D., Johnson, P.B., Caminiti, R., 1997. Premotor and parietal cortex: corticocortical connectivity and combinatorial computations. Annu. Rev. Neurosci. 20, 25–42.
Woolrich, M.W., Jbabdi, S., Patenaude, B., Chappell, M., Makni, S., Behrens, T., Beckmann, C., Jenkinson, M., Smith, S.M., 2009. Bayesian analysis of neuroimaging data in FSL. Neuroimage 45, S173–S186.
Ziemann, U., Siebner, H.R., 2015. Inter-subject and inter-session variability of plasticity induction by non-invasive brain stimulation: boon or bane? Brain Stimul. 8, 662–663.